

# QSAR study on permeability of hydrophobic compounds with artificial membranes

Masaaki Fujikawa,<sup>a</sup> Kazuya Nakao,<sup>b</sup> Ryo Shimizu<sup>b</sup> and Miki Akamatsu<sup>a,\*</sup>

<sup>a</sup>Division of Environmental Science and Technology, Graduate School of Agriculture, Kyoto University, Kyoto 606-8502, Japan

<sup>b</sup>Tanabe Seiyaku Co., Ltd, Osaka 532-8505, Japan

Received 19 February 2007; revised 12 March 2007; accepted 12 March 2007

Available online 16 March 2007

**Abstract**—We previously reported a classical quantitative structure–activity relationship (QSAR) equation for permeability coefficients ( $P_{\text{app-pampa}}$ ) by parallel artificial membrane permeation assay (PAMPA) of structurally diverse compounds with simple physicochemical parameters, hydrophobicity at a particular pH ( $\log P_{\text{oct}}$  and  $|\text{p}K_{\text{a}} - \text{pH}|$ ), hydrogen-accepting ability ( $SA_{\text{HA}}$ ), and hydrogen-donating ability ( $SA_{\text{HD}}$ ); however, desipramine, imipramine, and testosterone, which have high  $\log P_{\text{oct}}$  values, were excluded from the derived QSAR equation because their measured  $P_{\text{app-pampa}}$  values were lower than calculated. In this study, for further investigation of PAMPA permeability of hydrophobic compounds, we experimentally measured the  $P_{\text{app-pampa}}$  of more compounds with high hydrophobicity, including several pesticides, and compared the measured  $P_{\text{app-pampa}}$  values with those calculated from the QSAR equation. As a result, compounds having a calculated  $\log P_{\text{app-pampa}} > -4.5$  showed lower measured  $\log P_{\text{app-pampa}}$  than calculated because of the barrier of the unstirred water layer and the membrane retention of hydrophobic compounds. The bilinear QSAR model explained the PAMPA permeability of the whole dataset of compounds, whether hydrophilic or hydrophobic, with the same parameters as the equation in the previous study. In addition, PAMPA permeability coefficients correlated well with Caco-2 cell permeability coefficients. Since Caco-2 cell permeability is effective for the evaluation of human oral absorption of compounds, the proposed bilinear model for PAMPA permeability could be useful for not only effective screening for several drug candidates but also the risk assessment of chemicals and agrochemicals absorbed by humans.

© 2007 Elsevier Ltd. All rights reserved.

## 1. Introduction

In recent years, in vitro methods for predicting oral drug absorption have progressed. In vitro models of intestinal absorption generally focus on determining membrane permeability using Caco-2 cells, MDCK cells, artificial membranes, and immobilized artificial membrane (IAM) columns.<sup>1</sup> The parallel artificial membrane permeation assay (PAMPA), proposed by Kansy et al. in 1998,<sup>2</sup> is a high throughput in vitro assay system that evaluates transcellular permeation. In PAMPA, a 96-well microtiter plate completely filled with aqueous buffer solutions is covered with a hydrophobic filter coated with lipids in an organic solvent solution in a sandwich construction.<sup>2</sup> The PAMPA permeability of several drugs has been evaluated using various lipids dissolved

in organic solvents, such as an egg lecithin in *n*-dodecane<sup>2,3</sup> or 1,9-decadiene,<sup>4–6</sup> the composition of the lipid membrane that mimics the intestinal brush border membrane in 1,7-octadiene (Bio-mimetic PAMPA),<sup>7–9</sup> the porcine polar brain lipid in dodecane,<sup>10</sup> 100% *n*-hexadecane (HDM-PAMPA),<sup>11</sup> diolphosphatidylcholine in dodecane (DOPC-PAMPA)<sup>12</sup>, and a phospholipid mixture in dodecane (Double-Sink PAMPA).<sup>12</sup> The PAMPA is used to screen for human intestinal absorption in pharmaceutical research because several papers indicated that PAMPA permeability is correlated with both Caco-2 cell permeability and human intestinal absorption.<sup>2,3,5–7,9,13–16</sup> PAMPA is also applicable for predicting passive blood–brain penetration<sup>10</sup> and human skin permeability.<sup>17</sup>

In our previous study,<sup>6</sup> we reported a classical QSAR equation for PAMPA permeability coefficients ( $P_{\text{app-pampa}}$ ) of structurally diverse compounds with simple physicochemical parameters,  $\log P_{\text{oct}}$ , where  $P_{\text{oct}}$  is the partition coefficient in the 1-octanol/water system, the absolute value of the difference between the  $\text{p}K_{\text{a}}$

**Keywords:** PAMPA; Unstirred water layer; Membrane retention; Structure–property relationships; Bilinear model.

\* Corresponding author. Tel./fax: +81 75 753 6489; e-mail: [akamatsu@kais.kyoto-u.ac.jp](mailto:akamatsu@kais.kyoto-u.ac.jp)

value of the compound and the experimental pH 7.3,  $|\text{p}K_{\text{a}} - \text{pH}|$ , the surface area occupied by the hydrogen-bond acceptor and donor atoms of each modeled conformer,  $SA_{\text{HA}}$ , and  $SA_{\text{HD}}$ ; however, desipramine, imipramine, and testosterone, having high  $\log P_{\text{oct}}$ , were excluded from the QSAR equation because their measured  $P_{\text{app-pampa}}$  values were lower than calculated. Although we attempted the bilinear analysis of PAMPA permeability coefficients including these three compounds, it was difficult to obtain a statistically significant equation because there were few hydrophobic compounds in the dataset. Since many chemicals and agrochemicals used widely are hydrophobic, it is inevitable that humans are exposed to these hydrophobic chemicals as residues in food and water, or in occupational use;<sup>18</sup> therefore, it is desirable to predict exposure using in vitro or in silico methods such as PAMPA.

In the present study, we experimentally measured the  $P_{\text{app-pampa}}$  of more compounds which have particularly high apparent hydrophobicity at the experimental pH, including several pesticides. Then, the  $P_{\text{app-pampa}}$  of the compounds, including the hydrophobic compounds, was analyzed using the QSAR approach to investigate whether other physicochemical parameters were significant in determining PAMPA permeability of the hydrophobic compounds. We also examined the effect of the unstirred water layer (UWL) and membrane retention on PAMPA permeability. Furthermore, PAMPA permeability of the hydrophobic compounds was compared with their Caco-2 cell permeability to investigate whether PAMPA is applicable for high-throughput evaluation to predict the exposure of humans to hydrophobic chemicals and agrochemicals, as well as drugs.

## 2. Results

### 2.1. Permeability with artificial membranes

Table 1 shows the permeability coefficient through an artificial membrane,  $P_{\text{app-pampa}}$  values of added 22 chemicals and 15 agrochemicals with the data reported previously.<sup>6</sup> We used Tris-HCl buffer (pH 7.3) containing 5–30% DMSO for the measurement of PAMPA permeability (5% DMSO: imidacloprid and 21 chemicals except pyrene; 20% DMSO: 13 agrochemicals except biphenyl and imidacloprid; 30% DMSO: biphenyl and pyrene). The  $\log P_{\text{app-pampa}}$  values of added compounds were in the range of  $-5.95$  (biphenyl) to  $-4.12$  (aniline). The relative standard deviation values of  $P_{\text{app-pampa}}$  of added compounds were less than 50%, except for biphenyl (57%) and salithion (66%).

### 2.2. Classical QSAR equations for the $\log P_{\text{app-pampa}}$

We previously formulated a classical QSAR Equation 1 for the PAMPA permeability coefficients of structurally diverse compounds with simple physicochemical parameters.<sup>6</sup> The  $\log P_{\text{app-pampa}}$  values of the 37 added compounds were calculated according to Eq. 1. The calculated values are listed in Table 1.

$$\begin{aligned} \log P_{\text{app-pampa}} = & 0.43 (\pm 0.09) \log P_{\text{oct}} \\ & - 0.25 (\pm 0.08) |\text{p}K_{\text{a}} - \text{pH}| \\ & - 1.07 (\pm 0.49) SA_{\text{HA}} \\ & - 1.00 (\pm 0.42) SA_{\text{HD}} - 4.98 (\pm 0.31) \end{aligned} \quad (1)$$

$$n = 57, s = 0.33, r^2 = 0.76, q^2 = 0.72$$

where,  $n$  is the number of compounds,  $s$  is the standard deviation,  $r$  is the correlation coefficient,  $q$  is the cross-validated (leave-one-out) correlation coefficient, and the figures in parentheses are 95% confidence intervals.

Figure 1 shows the relationship between measured and calculated  $\log P_{\text{app-pampa}}$  values of previous and added compounds. For compounds with calculated  $\log P_{\text{app-pampa}} \leq -4.5$ , their measured  $\log P_{\text{app-pampa}}$  values correlated well with the calculated values. On the other hand, for compounds which have calculated  $\log P_{\text{app-pampa}} > -4.5$ , the measured  $\log P_{\text{app-pampa}}$  was lower than calculated. The difference between the measured and calculated values enlarged consistently with the increase of the calculated  $\log P_{\text{app-pampa}}$  values.

Based on this observation, the dataset was divided into two groups; compounds having low calculated  $\log P_{\text{app-pampa}}$  values ( $\leq -4.5$ ) (Group 1: 71 compounds) and compounds having high calculated  $\log P_{\text{app-pampa}}$  values ( $> -4.5$ ) (Group 2: 26 compounds). We separately formulated QSAR equations for Group 1 and Group 2.

Group 1 (calculated  $\log P_{\text{app-pampa}} \leq -4.5$ )

$$\begin{aligned} \log P_{\text{app-pampa}} = & 0.42 (\pm 0.09) \log P_{\text{oct}} \\ & - 0.28 (\pm 0.07) |\text{p}K_{\text{a}} - \text{pH}| \\ & - 1.20 (\pm 0.47) SA_{\text{HA}} \\ & - 1.11 (\pm 0.40) SA_{\text{HD}} - 4.79 (\pm 0.30) \end{aligned} \quad (2)$$

$$n = 71, s = 0.35, r^2 = 0.76, q^2 = 0.72.$$

Group 2 (calculated  $\log P_{\text{app-pampa}} > -4.5$ )

$$\begin{aligned} \log P_{\text{app-pampa}} = & -0.40 (\pm 0.16) \log P_{\text{oct}} \\ & + 0.24 (\pm 0.15) |\text{p}K_{\text{a}} - \text{pH}| \\ & - 3.68 (\pm 0.51) \end{aligned} \quad (3)$$

$$n = 26, s = 0.30, r^2 = 0.54, q^2 = 0.42.$$

The  $\log P_{\text{oct}}$ ,  $|\text{p}K_{\text{a}} - \text{pH}|$ ,  $SA_{\text{HA}}$ , and  $SA_{\text{HD}}$  were significant in determining variations in PAMPA permeability coefficients in Eq. 2 in a similar manner to Eq. 1. In Eqs. 1 and 2, the coefficients of the corresponding terms and intercept were identical within 95% confidence intervals. In Eq. 3, the significant parameters were only  $\log P_{\text{oct}}$  and  $|\text{p}K_{\text{a}} - \text{pH}|$ . The introduction of any other physicochemical parameters did not improve Eq. 3. It will be probably due to the small number of compounds in Group 2. It is not at least due to the experimental error because the deviation in  $\log P_{\text{app-pampa}}$  of Group 2 was similar to that of Group 1.

**Table 1.** Permeability coefficients and membrane retention of tested compounds and their QSAR parameters

No.	Compound	Group <sup>a</sup>	$P_{\text{app-pampa}}^b$ ( $\times 10^{-6}$ ) (cm/s)	$\log P_{\text{app-pampa}}$			$P_{\text{app-pampa}}$ (stir) <sup>c</sup> ( $\times 10^{-6}$ ) (cm/s)		$\log P_{\text{app-pampa}}$ (stir)	$\log P_{\text{app-Caco2}}^f$	Membrane retention (%)	$\log P_{\text{oct}}$	ClogP	pK <sub>a</sub> – pH	$PSA^g$	$SA_{\text{HA}}^h$	$SA_{\text{HD}}^i$	MW
				Measured	Calculated <sup>c</sup>	Calculated <sup>d</sup>	measured											
Peptide related compounds																		
1	Boc-Trp	1	1.84 [0.99]	–5.74	–5.77	–5.79	—	—	—	–5.67	—	2.65	2.80	3.60	0.995	0.557	0.438	304
2	Cbz-Trp	1	2.82 [0.95]	–5.55	–5.62	–5.57	—	—	—	–5.80	—	3.20	3.25	3.60	1.076	0.637	0.439	338
3	Fmoc-Trp	1	12.75 [1.36]	–4.89	–4.90	–5.25	—	—	—	–4.76	—	4.93	5.08	3.60	1.097	0.658	0.439	426
4	Trp-NH <sub>2</sub>	1	2.73 [0.27]	–5.56	–5.90	–5.90	—	—	—	—	—	0.30	–0.15	0.20	0.982	0.320	0.661	203
5	Ac-Trp-NH <sub>2</sub>	1	1.92 [0.36]	–5.72	–5.74	–5.65	—	—	—	–5.63	—	0.42	–0.19	0.00	0.907	0.419	0.488	245
6	Gly-Trp-NH <sub>2</sub>	1	0.42 [0.21]	–6.38	–6.59	–6.59	—	—	—	—	—	–0.48	–1.76	0.00	1.363	0.530	0.832	260
7	Phe-Trp-NH <sub>2</sub>	1	5.98 [0.61]	–5.22	–5.77	–5.67	—	—	—	—	—	1.38	1.01	0.00	1.345	0.513	0.833	350
8	Trp-Ala-Val-NH <sub>2</sub>	1	0.24 [0.05]	–6.62	–6.45	–6.34	—	—	—	—	—	0.40	0.26	0.00	1.593	0.663	0.930	373
9	Ac-Trp-Val-NH <sub>2</sub>	1	0.66 [0.48]	–6.18	–6.03	–5.88	—	—	—	–6.77	—	0.73	0.48	0.00	1.320	0.635	0.685	344
10	Ac-D-Trp-Val-NH <sub>2</sub>	1	0.73 [0.73]	–6.14	–5.92	–5.80	—	—	—	–6.92	—	0.65	0.48	0.00	1.184	0.541	0.643	344
11	Ac-Tyr-Leu-NH <sub>2</sub>	1	0.29 [0.11]	–6.54	–6.06	–5.97	—	—	—	—	—	0.32	0.35	0.00	1.183	0.527	0.657	335
12	Ac-Tyr-Phe-NH <sub>2</sub>	1	0.12 [0.10]	–6.92	–6.18	–6.01	—	—	—	—	—	0.54	0.31	0.00	1.381	0.713	0.668	369
13	Cyclo(-Trp-Gly)	1	0.97 [0.70]	–6.02	–5.95	–5.86	—	—	—	–6.12	—	0.07	–0.32	0.00	0.961	0.509	0.452	243
14	Cyclo(-Trp-Tyr)	1	0.68 [0.70]	–6.17	–5.75	–5.57	—	—	—	—	—	1.11	1.47	0.00	1.201	0.621	0.580	349
15	Cyclo(-Trp-Trp)	1	9.10 [1.99]	–5.04	–5.26	–5.26	—	—	—	–5.92	—	2.04	2.13	0.00	1.119	0.533	0.586	372
16	Indole	2	31.91 [7.17]	–4.50	–4.29	–4.43	—	—	—	–4.24	—	2.14	2.13	0.00	0.228	0.079	0.149	117
17	Tryptophol	1	19.11 [2.02]	–4.72	–4.82	–4.77	—	—	—	–4.24	—	1.54	1.32	0.00	0.491	0.196	0.295	147
18	Tryptamine	1	5.42 [1.24]	–5.27	–5.68	–5.89	—	—	—	—	—	1.35	1.42	2.90	0.551	0.124	0.427	160
19	Indole-3-acetamide	1	6.18 [0.56]	–5.21	–5.37	–5.30	—	—	—	–4.23	—	0.75	0.44	0.00	0.693	0.280	0.414	174
20	Indole-3-carboxylic acid	1	0.79 [0.05]	–6.10	–5.62	–5.67	—	—	—	–4.56	—	1.99	2.13	3.10	0.689	0.398	0.291	161
21	Indole-3-acetic acid	1	0.40 [0.02]	–6.40	–5.79	–5.91	—	—	—	–4.85	—	1.41	1.40	3.00	0.641	0.362	0.279	175
22	Indole-3-propionic acid	1	2.10 [0.73]	–5.68	–5.56	–5.60	—	—	—	–4.67	—	1.75	1.89	2.60	0.656	0.366	0.290	189
Drugs																		
23	Acebutolol	1	0.36 [0.04]	–6.44	–5.82	–5.76	2.64 [0.87]	–5.58	—	–6.29	—	1.71	1.70	2.11	1.006	0.582	0.424	336
24	Acetaminophen	1	0.91 [0.27]	–6.04	–5.41	–5.32	2.22 [1.04]	–5.65	—	—	—	0.51	0.49	0.00	0.624	0.331	0.293	151
25	Alprenolol	1	11.50 [0.86]	–4.94	–4.82	–4.83	61.38 [10.85]	–4.21	—	–4.60	—	2.89	2.65	2.30	0.493	0.211	0.281	249
26	Antipyrine	1	2.87 [0.12]	–5.54	–5.18	–5.09	10.08 [4.13]	–5.00	—	—	—	0.23	0.20	0.00	0.279	0.279	0.000	188
27	Caffeine	1	3.92 [1.28]	–5.41	–5.75	–5.56	15.95 [3.62]	–4.80	—	–4.51	—	–0.07	–0.06	0.00	0.695	0.695	0.000	194
28	Chloramphenicol	1	3.89 [0.39]	–5.41	–5.73	–5.47	5.75 [0.48]	–5.24	—	—	—	1.14	1.28	0.00	1.181	0.790	0.391	323
29	Clonidine	1	10.41 [1.20]	–4.98	–5.03	–5.00	11.44 [1.82]	–4.94	—	–4.66	—	1.43	1.41	0.75	0.468	0.182	0.286	230
30	Corticosterone	1	16.81 [2.10]	–4.77	–4.96	–4.89	34.25 [2.21]	–4.47	—	–4.67	—	1.94	2.32	0.00	0.777	0.517	0.261	346
31	Coumarin	1	27.99 [3.09]	–4.55	–4.74	–4.59	276.83 [33.70]	–3.56	—	—	—	1.39	1.41	0.00	0.330	0.330	0.000	146
32	Dexamethasone	1	4.26 [0.36]	–5.37	–5.16	–5.12	11.26 [1.96]	–4.95	—	–4.91	—	2.01	1.75	0.00	1.007	0.587	0.420	392
33	Diltiazem	1	19.21 [1.61]	–4.72	–4.64	–4.68	123.70 [13.41]	–3.91	—	—	—	2.80	3.65	0.76	0.783	0.628	0.000	415
34	Furosemide	1	0.34 [0.05]	–6.47	–6.60	–6.62	0.57 [0.44]	–6.25	—	—	—	2.03	1.87	3.96	1.443	0.868	0.570	331
35	Hydrochlorothiazide	1	0.20 [0.02]	–6.69	–6.59	–6.38	0.29 [0.15]	–6.54	—	–6.29	—	–0.07	–0.40	0.00	1.525	0.964	0.549	298
36	Hydrocortisone	1	3.53 [0.82]	–5.45	–5.28	–5.13	8.51 [3.16]	–5.07	—	–4.85	—	1.61	1.70	0.00	0.951	0.560	0.391	362
37	Ibuprofen	1	21.15 [7.85]	–4.67	–4.66	–4.66	72.11 [25.37]	–4.14	—	—	—	3.50	3.68	2.92	0.430	0.299	0.131	206
38	Imipramine	2	19.36 [3.92]	–4.71	–3.67	–4.53	63.77 [12.99]	–4.20	—	—	44	4.44	5.04	2.10	0.073	0.073	0.000	280
39	Ketoprofen	1	2.84 [0.14]	–5.55	–5.04	–4.97	4.01 [0.81]	–5.40	—	—	—	3.12	2.76	3.01	0.615	0.471	0.144	254
40	Labetalol	1	6.60 [0.56]	–5.18	–5.29	–5.32	5.64 [1.01]	–5.25	—	–5.03	—	3.09	2.50	2.10	1.085	0.416	0.669	328
41	Metoprolol	1	7.93 [3.91]	–5.10	–5.43	–5.45	14.35 [5.89]	–4.84	—	–4.63	—	1.88	1.35	2.45	0.622	0.341	0.281	267
42	Nadolol	1	0.71 [0.50]	–6.15	–6.25	–6.39	32.67 [14.42]	–4.49	—	–5.41	—	0.71	0.38	2.37	0.957	0.409	0.549	309
43	Naproxen	1	5.01 [0.36]	–5.30	–4.93	–4.89	5.48 [2.02]	–5.26	—	—	—	3.34	2.82	3.29	0.532	0.401	0.130	230

44	Norfloxacin	1	0.19	[0.08]	−6.71	−6.79	−6.98	0.18	[0.08]	−6.74	—	—	−1.03	−0.99	2.08	0.808	0.560	0.248	319
45	Oxprenolol	1	14.64	[6.07]	−4.83	−5.30	−5.28	9.36	[2.35]	−5.03	—	—	2.10	2.09	2.30	0.624	0.362	0.262	265
46	Pindolol	1	4.91	[1.53]	−5.31	−5.48	−5.53	1.42	[0.64]	−5.85	−4.78	—	1.75	1.67	2.24	0.670	0.257	0.413	248
47	Practolol	1	1.06	[0.09]	−5.98	−6.05	−6.13	0.37	[0.37]	−6.43	—	—	0.79	0.75	2.10	0.858	0.435	0.423	266
48	Prednisolone	1	3.37	[0.41]	−5.47	−5.30	−5.16	2.99	[0.80]	−5.52	—	—	1.62	1.38	0.00	0.982	0.561	0.420	360
49	Propranolol	1	26.33	[4.02]	−4.58	−4.77	−4.79	38.37	[6.26]	−4.42	−4.66	—	2.98	2.75	2.30	0.483	0.209	0.274	258
50	Ranitidine	1	0.88	[0.10]	−6.05	−6.05	−5.94	3.00	[1.16]	−5.52	−6.31	—	0.27	0.63	0.88	1.095	0.699	0.222	314
51	Salicylic acid	1	1.21	[0.60]	−5.92	−5.85	−5.99	4.90	[2.48]	−5.31	−4.66	—	2.26	2.19	4.32	0.730	0.444	0.286	138
52	Testosterone	2	11.20	[3.10]	−4.95	−4.02	−5.02	136.42	[33.63]	−3.87	−4.60	5	3.32	3.22	0.00	0.447	0.307	0.140	288
53	Theophylline	1	4.84	[1.21]	−5.31	−5.78	−5.62	2.61	[0.97]	−5.58	—	—	−0.02	−0.06	0.00	0.746	0.611	0.135	180
54	Trimethoprim	1	3.14	[0.42]	−5.50	−5.85	−5.67	4.18	[1.56]	−5.38	—	—	0.91	0.88	0.00	1.219	0.658	0.561	290
55	Verapamil	2	23.02	[3.74]	−4.64	−4.46	−4.93	110.44	[21.23]	−3.96	—	—	3.79	4.47	1.36	0.717	0.717	0.000	455
56	Aminopyrine	1	17.29	[1.03]	−4.76	−4.83	−4.70	72.31	[4.93]	−4.14	−4.44	—	1.00	0.57	0.00	0.266	0.266	0.000	231
57	Desipramine	2	16.98	[1.70]	−4.77	−4.05	−4.41	156.14	[7.56]	−3.81	−4.61	2	4.54	4.47	3.35	0.185	0.048	0.137	266
58	Phenytoin	1	38.53	[10.32]	−4.41	−4.75	−4.84	11.88	[4.89]	−4.93	−4.57	—	2.26	2.08	0.00	0.708	0.441	0.267	252
59	Piroxicam	1	10.87	[1.76]	−4.96	−5.78	−5.62	19.23	[1.89]	−4.72	−4.45	—	1.98	1.89	2.23	1.045	0.798	0.241	331
60	Pirenzepine	1	0.89	[0.19]	−6.05	−5.92	−5.82	0.82	[0.20]	−6.09	−6.36	—	0.10	0.17	0.70	0.765	0.618	0.147	351
<i>Chemicals</i>																			
61	2,4-Dichlorophenol	2	11.86	[1.55]	−4.93	−3.96	−4.76	127.19	[30.23]	−3.90	—	42	3.06	2.96	0.00	—	0.139	0.144	163
62	2,4-Dimethylphenol	2	24.34	[4.70]	−4.61	−4.27	−4.48	262.87	[44.40]	−3.58	—	20	2.30	2.47	0.00	—	0.131	0.142	122
63	2,5-Dichloronitrobenzene	2	7.78	[2.07]	−5.11	−4.19	−4.83	80.65	[29.59]	−4.09	—	44	3.03	3.11	0.00	—	0.477	0.000	192
64	2-Chloroaniline	2	33.14	[4.77]	−4.48	−4.48	−4.55	245.89	[58.51]	−3.63	—	21	1.90	1.91	0.00	—	0.045	0.266	128
65	2-Chlorophenol	2	50.00	[6.63]	−4.30	−4.35	−4.47	15.21	[4.65]	−4.82	—	18	2.15	2.16	0.00	—	0.139	0.144	139
66	2-Methylphenol	2	52.10	[11.17]	−4.28	−4.42	−4.47	295.00	[160.52]	−3.53	—	3	1.95	1.97	0.00	—	0.130	0.142	108
67	2-Nitroaniline	1	28.60	[2.67]	−4.54	−4.95	−4.86	229.36	[21.87]	−3.64	—	14	1.85	1.80	0.00	—	0.479	0.253	138
68	2-Nitrophenol	1	56.96	[7.77]	−4.24	−4.99	−4.83	216.50	[30.16]	−3.66	—	20	1.79	1.85	0.08	—	0.574	0.142	139
69	3-Chloroaniline	2	36.69	[6.61]	−4.44	−4.49	−4.55	261.43	[92.75]	−3.58	—	7	1.88	1.91	0.00	—	0.046	0.266	128
70	3-Nitroaniline	1	21.56	[1.32]	−4.67	−5.20	−5.03	195.69	[13.78]	−3.70	—	0.3	1.37	1.26	0.00	—	0.511	0.265	138
71	3-Nitrophenol	1	17.09	[3.04]	−4.77	−4.90	−4.81	69.41	[7.00]	−4.16	—	11	2.00	1.85	0.00	—	0.598	0.144	139
72	4-Chloroaniline	2	41.75	[4.19]	−4.38	−4.49	−4.55	258.24	[25.83]	−3.59	—	8	1.88	1.91	0.00	—	0.046	0.266	128
73	4-Cyanophenol	1	17.04	[5.67]	−4.77	−4.84	−4.72	22.26	[2.04]	−4.65	—	10	1.60	1.60	0.00	—	0.379	0.144	119
74	4-Nitroaniline	1	20.79	[7.21]	−4.68	−5.20	−5.02	122.27	[9.27]	−3.91	—	1	1.39	1.26	0.00	—	0.512	0.265	138
75	Aniline	1	75.92	[9.96]	−4.12	−4.91	−4.89	305.58	[25.74]	−3.51	—	2	0.90	0.92	0.00	—	0.046	0.266	93
76	Diethyl phtalate	1	15.05	[6.59]	−4.82	−4.51	−4.67	46.86	[44.66]	−4.33	—	37	2.47	2.62	0.00	—	0.557	0.000	222
77	Dimethyl phtalate	1	43.32	[10.07]	−4.36	−4.91	−4.70	157.68	[33.94]	−3.80	—	13	1.56	1.56	0.00	—	0.563	0.000	194
78	Diphenylamine	2	3.10	[0.97]	−5.51	−3.68	−4.95	15.02	[2.33]	−4.82	−4.40	53	3.50	3.62	0.00	—	0.053	0.149	169
79	Hydroquinone	1	7.31	[2.13]	−5.14	−5.25	−5.18	4.60	[0.89]	−5.34	—	2	0.59	0.81	0.00	—	0.241	0.262	110
80	Phenol	1	47.05	[4.98]	−4.33	−4.64	−4.58	147.10	[41.89]	−3.83	—	8	1.47	1.48	0.00	—	0.136	0.144	94
81	Pyrene	2	2.22	[0.97]	−5.65	−2.88	−5.61	47.63	[17.12]	−4.32	—	58	4.88	4.95	0.00	—	0.000	0.000	202
82	Diphenylamine-2-carboxylic acid	2	13.83	[1.93]	−4.86	−4.49	−4.66	24.30	[0.52]	−4.61	—	—	4.36	—	3.15	—	0.493	0.071	213
83	Atrazine	1	29.18	[1.97]	−4.53	−4.74	−5.03	72.11	[8.17]	−4.14	−4.39	3	2.61	2.5	0.00	—	0.547	0.295	216
84	Benthocarb	2	20.55	[2.92]	−4.69	−3.69	−4.81	92.93	[34.37]	−4.03	—	23	3.42	3.51	0.00	—	0.168	0.000	258
85	Biphenyl	2	1.12	[0.64]	−5.95	−3.26	−5.05	53.28	[21.24]	−4.27	—	69	4.01	4.03	0.00	—	0.000	0.000	154
86	BPMC	2	12.42	[3.15]	−4.91	−4.21	−4.72	131.01	[47.16]	−3.88	—	9	2.78	2.82	0.00	—	0.264	0.146	207
87	Diazinon	2	5.21	[2.12]	−5.28	−4.19	−5.06	31.14	[24.69]	−4.51	−4.32	65	3.30	3.5	0.00	—	0.587	0.000	305
88	DMTP	1	10.78	[3.79]	−4.97	−4.59	−4.74	46.88	[19.03]	−4.33	−4.32	40	2.50	2.77	0.00	—	0.643	0.000	302
89	IBP	2	11.71	[5.49]	−4.93	−4.01	−4.85	361.96	[223.88]	−3.44	−4.28	27	3.21	3.02	0.00	—	0.382	0.000	288
90	Imidacloprid	1	4.52	[0.28]	−5.34	−5.72	−5.44	5.21	[0.13]	−5.31	—	4	0.59	0.67	0.00	—	0.812	0.126	256

(continued on next page)

Table 1 (continued)

No.	Compound	Group <sup>a</sup>	$P_{app-pampa}$ ( $\times 10^{-6}$ ) (cm/s)	$\log P_{app-pampa}$		$P_{app-pampa}$ ( $\times 10^{-6}$ ) (cm/s)	$\log P_{app-pampa}$ (stir) measured	$\log P_{app-pampa}$ (stir) measured	$\log P_{app-Caco2}$ <sup>f</sup>	Membrane retention (%)	$\log P_{oct}$	$\log P_{oct}$	$pK_a - pH$	$PSA^g$	$SA_{HA}^h$	$SA_{HD}^i$	$MW$	
				Measured	Calculated <sup>c</sup>													Calculated <sup>d</sup>
91	MEP	2	2.85 [1.03]	-5.55	-4.40	-5.20	12.90	[4.29]	-4.89	—	47	3.30	3.21	0.00	—	0.787	0.000	277
92	Salithion	2	9.39 [6.23]	-5.03	-4.26	-4.61	43.87	[18.82]	-4.36	—	43	2.67	2.67	0.00	—	0.397	0.000	216
93	Tebufenozide	2	15.74 [2.46]	-4.80	-3.77	-5.69	—	—	—	-4.44	3	4.25	—	0.00	—	0.449	0.132	353
94	Methoxyfenozide	2	19.06 [2.57]	-4.72	-4.11	-5.42	—	—	—	-4.33	0	3.70	—	0.00	—	0.553	0.132	368
95	Halofenozide	2	17.24 [2.14]	-4.76	-4.21	-5.06	—	—	—	—	5	3.22	—	0.00	—	0.448	0.132	331
96	Chromafenozide	1	16.69 [1.83]	-4.78	-4.54	-4.88	—	—	—	—	12	2.70	—	0.00	—	0.546	0.133	394
97	RH-5849	1	16.52 [1.18]	-4.78	-4.52	-4.71	—	—	—	-4.34	0.3	2.45	—	0.00	—	0.432	0.129	296

<sup>a</sup> Compounds were classified into two groups based on the  $\log P_{app-pampa}$  values calculated by Eq. 1; compounds having low calculated  $\log P_{app-pampa}$  values ( $\leq -4.5$ ) (Group 1) and compounds having high calculated  $\log P_{app-pampa}$  values ( $> -4.5$ ) (Group 2).

<sup>b</sup> The measurement was repeated at least four times. Values in parentheses are the standard deviation. Data of the compound No. 1–60 are from Refs. 5, 6.

<sup>c</sup> The values were predicted by Eq. 1.

<sup>d</sup> The values were predicted by Eq. 4 (bilinear equation).

<sup>e</sup> PAMPA permeability coefficient under the stirred condition. Values in parentheses are the standard deviation.

<sup>f</sup> Caco-2 permeability coefficients (apical to basolateral). Data of the compound No. 1–22 and 23–60 are from Refs. 6, 38, respectively.

<sup>g</sup> Van der Waals surface area ( $\text{\AA}^2 \times 1/100$ ) occupied by polar atoms. Data of the compound No. 1–60 are from Refs. 5, 6.

<sup>h</sup> Van der Waals surface area ( $\text{\AA}^2 \times 1/100$ ) occupied by hydrogen-bond acceptor atoms. Data of the compound No. 1–60 are from Refs. 5, 6.

<sup>i</sup> Van der Waals surface area ( $\text{\AA}^2 \times 1/100$ ) occupied by hydrogen-bond donor atoms. Data of the compound No. 1–60 are from Refs. 5, 6.

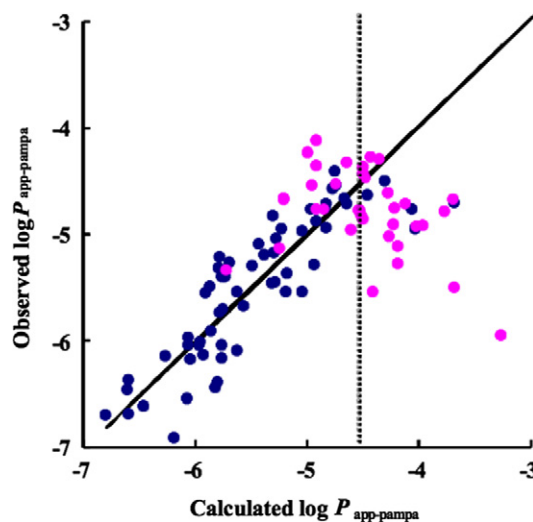


Figure 1. The relationship between observed and calculated artificial membrane permeability coefficients of tested compounds. The values of  $\log P_{app-pampa}$  were calculated from Eq. 1. ●: previous compound set (60 compounds), ●: added compound set (37 compounds).

As discussed in Section 3.2.2,  $(\log P_{oct} - \alpha[pK_a - pH])$  represents apparent hydrophobicity,  $\log P_{app}$ , at a particular pH when the partition of ion-pair complexes to 1-octanol cannot be neglected. The ‘ $\alpha$ ’ value is variable depending on the experimental conditions such as the components of buffer solutions. The similarity of ‘ $\alpha$ ’ values in Eqs. 1–3 ( $\alpha = -[\text{the coefficient of the } [pK_a - pH] \text{ term/the coefficient of the } \log P_{oct} \text{ term}]$ : 0.58, 0.67, and 0.60, respectively) indicates that PAMPA permeability varies with  $\log P_{app}$  at pH 7.3. Therefore, further bilinear QSAR analysis for PAMPA permeability of the combined set of 97 compounds in Groups 1 and 2 was performed using the parameter  $\log P_{app}$ . The bilinear model is a non-linear model developed by Kubinyi<sup>19</sup> and is applicable to the bi-phase (linear ascending and descending) dependence of biological activity on hydrophobic characteristics. We adopted the most reliable value, 0.67, in Eq. 2 as ‘ $\alpha$ ’ and obtained Eq. 4.

$$\log P_{app-pampa} = 0.53 (\pm 0.10) \log P_{app} - 1.18 (\pm 0.25) \log (\beta 10^{\log P_{app}} + 1) - 0.74 (\pm 0.35) SA_{HA} - 1.13 (\pm 0.39) SA_{HD} - 5.00 (\pm 0.24) \quad (4)$$

$$n = 97, s = 0.36, r^2 = 0.72, q^2 = 0.68, \log P_{app}(\text{optimum}) = 2.08, \log \beta = -2.17.$$

According to Eq. 4, PAMPA permeability increases with the apparent hydrophobicity of compounds up to the  $\log P_{app}$  ( $= \log P_{oct} - 0.67[pK_a - pH]$ ) value of 2.08 with a slope of 0.53, and then linearly decreases for compounds having high apparent hydrophobicity (slope of the  $\log P_{app}$  term  $= 0.53 - 1.18 = -0.65$ ). Significant parameters in addition to  $\log P_{app}$  in the bilinear model were  $SA_{HA}$  and  $SA_{HD}$ , as in Eq. 1. Thus, one good bilinear model which was useful for the pre-



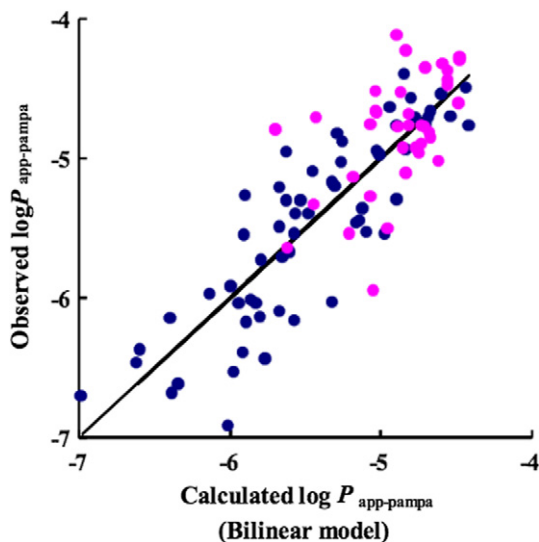


**Figure 2.** The relationship between observed and calculated artificial membrane permeability coefficients of 97 compounds. The values of  $\log P_{\text{app-pampa}}$  were calculated from Eq. 4 (bilinear model). ● previous compound set (60 compounds), ● added compound set (37 compounds).

diction of all tested compounds was derived. Figure 2 shows the relationship between the observed and calculated artificial membrane permeability coefficients of 97 compounds.

### 2.3. Permeability with artificial membranes under the stirred condition

The unstirred water layer (UWL) exists on both sides of the membrane surface, acting as a rate-limiting barrier for highly permeable compounds. Thus, the permeability of highly permeable compounds is affected by the thickness of the UWL.<sup>20</sup> Since the UWL can become thinner with vigorous stirring,<sup>12</sup> we measured  $P_{\text{app-pampa (stir)}}$ , the PAMPA permeability coefficient, under the stirred condition in the donor and acceptor solutions to examine the effect of the UWL on PAMPA permeability. Table 2 shows the  $\log P_{\text{app-pampa (stir)}}$  of desipramine, imipramine, testosterone, aminopyrine, verapamil, and ketoprofen at stirring speeds of 0, 100, 200, and 250 rpm. The PAMPA permeability values of ketoprofen, a moderately permeable compound (unstirred  $\log P_{\text{app-pampa}}$ : −5.55), did not change significantly at any

stirring speed. In contrast, the  $\log P_{\text{app-pampa (stir)}}$  values of other highly permeable compounds (unstirred  $\log P_{\text{app-pampa}}$  = −4.95 to −4.64) increased with the stirring speed.

Table 1 lists  $\log P_{\text{app-pampa (stir)}}$  of compounds at a stirring speed of 250 rpm. Compounds with a higher calculated  $\log P_{\text{app-pampa}}$  (>−4.5) showed a larger unstirred–stirred difference, [ $(\log P_{\text{app-pampa (stir)}}$  at a stirring speed of 250 rpm) − ( $\log P_{\text{app-pampa}}$  under the unstirred condition)]. For example, the PAMPA permeability of IBP (calculated value: −4.01), biphenyl (calculated value: −3.26), and pyrene (calculated value: −2.88) increased by 1.49, 1.68, and 1.33 log unit under the stirred condition, respectively. Bilinear QSAR analysis for  $\log P_{\text{app-pampa (stir)}}$  at a stirring speed of 250 rpm was performed using the parameter  $\log P_{\text{app}}$ . A good equation identical to Eq. 4 except for having a more gradual descending slope of the  $\log P_{\text{app}}$  term (−0.50 vs −0.65) was derived (equation not shown).

### 2.4. UWL permeability and intrinsic permeability of ionized compounds

We evaluated the UWL permeability coefficient ( $P_{\text{UWL}}$ ) and intrinsic artificial membrane permeability coefficient ( $P_0$ ) for 14 highly permeable compounds using the pH dependence method to determine the effect of the UWL on PAMPA permeability. The UWL permeability coefficient corresponds to the observed maximum permeability coefficient of a compound under the existence of the UWL on both sides of the membrane. The intrinsic artificial membrane permeability coefficient is the theoretical maximum membrane permeability coefficient of an ionizable compound in its uncharged form that could be reached if the UWL did not exist.<sup>21</sup> The  $\log P_{\text{UWL}}$  and the ‘flux’ ionization constant ( $\text{p}K_{\text{a}}^{\text{flux}}$ ), which refers to the pH value where the resistance to transport is 50% due to the artificial membrane barrier and 50% due to the UWL,<sup>21</sup> were estimated by the  $\log P_{\text{app-pampa-pH}}$  plot (Fig. 3). The  $\log P_0$  value was calculated using the estimated  $\log P_{\text{UWL}}$  and  $\text{p}K_{\text{a}}^{\text{flux}}$ , and  $\text{p}K_{\text{a}}$  of a compound (see Section 5.4). Figure 3 shows the profiles of  $\log P_{\text{app-pampa}}$  of desipramine (a base), ketoprofen (an acid), and testosterone (a non-ionized compound) over the range of pH 3–10. Other bases and acids showed similar profiles to desipramine and ketoprofen, respectively. Table 3 lists the  $\log P_{\text{UWL}}$ ,  $\log P_0$ , and  $\text{p}K_{\text{a}}^{\text{flux}}$  values of 14 compounds. The values of  $P_0$  and  $\text{p}K_{\text{a}}^{\text{flux}}$  of testosterone were not calculated because testosterone is a non-ionized compound, in which the  $\log P_{\text{app-pampa}}$  value ( $\approx \log P_{\text{UWL}}$ ) does not depend on pH. The  $\log P_{\text{UWL}}$  of the 14 highly permeable compounds was in the range of −4.95 to −4.44, similar to the measured  $\log P_{\text{app-pampa}}$ , as shown in Table 1. This indicated that the unstirred water layer is rate-limiting for the PAMPA permeability of these highly permeable compounds.

We examined the relationship between  $\log P_0$  and the physicochemical parameters of 13 compounds except testosterone (a non-ionized compound) and formulated a QSAR equation as follows:

**Table 2.** Permeability coefficients of compounds under the stirred condition

Compounds	$\log P_{\text{app-pampa}}$ 0 rpm <sup>a</sup>	$\log P_{\text{app-pampa (stir)}}$		
		100 rpm	200 rpm	250 rpm
Desipramine	−4.77	−4.15	−4.00	−3.81
Imipramine	−4.71	−4.52	−4.36	−4.20
Testosterone	−4.95	−4.29	−4.08	−3.87
Aminopyrine	−4.76	−4.41	−4.30	−4.14
Verapamil	−4.64	−4.31	−4.13	−3.96
Ketoprofen	−5.55	−5.55	−5.49	−5.40

<sup>a</sup>  $\log P_{\text{app-pampa}}$  (measured) in Table 1.

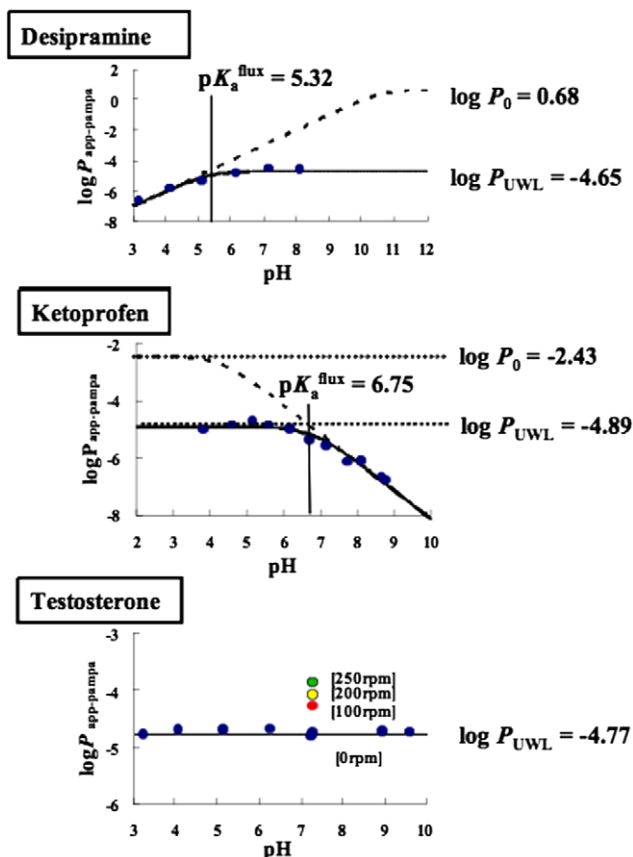


**Figure 3.** The profiles of artificial membrane permeability coefficients of desipramine, ketoprofen, and testosterone over a range of pH 3–10.

**Table 3.** Unstirred water layer and intrinsic permeability coefficients and the ‘flux’  $pK_a$

Compounds		$\log P_{UWL}$	$\log P_0$	$pK_a^{\text{flux}}$
Base	Aminopyrine	−4.62	−4.23	4.48
	Diltiazem	−4.64	−1.85	5.27
	Alprenolol	−4.70	−1.02	5.92
	Metoprolol	−4.95	−1.75	6.55
	Propranolol	−4.68	−1.57	6.49
	Desipramine	−4.65	0.68	5.32
	Imipramine	−4.65	1.23	3.52
	Verapamil	−4.68	−0.20	4.18
Acid	Ketoprofen	−4.89	−2.43	6.75
	Ibuprofen	−4.72	−1.15	7.95
	Salicylic acid	−4.62	−3.46	4.14
	Naproxen	−4.89	−0.49	8.41
	Piroxicam	−4.44	−2.08	7.43
Non-ionized	Testosterone	−4.77	—	—

$$\log P_0 = 1.34 (\pm 0.45) \log P_{\text{oct}} - 5.39 (\pm 1.39) \quad (5)$$

$n = 13, s = 0.71, r^2 = 0.80, q^2 = 0.73.$

The terms  $SA_{HA}$  and  $SA_{HD}$  were not significant in Eq. 5, probably due to the small number of compounds. The coefficient of the  $\log P_{\text{oct}}$  term in Eq. 5 was 1.34, larger than the corresponding coefficient in Eqs. 1–3 (0.43–0.53).

**Table 4.** Caco-2 permeability coefficients of chemicals and agrochemicals

Compounds		$\log P_{\text{app-caco2}} (A \rightarrow B)$	$\log P_{\text{app-caco2}} (B \rightarrow A)$
Chemical	Diphenylamine	−4.40	−4.35
Agrochemical	Atrazine	−4.39	−4.45
	Diazinon	−4.32	−4.42
	DMTP	−4.32	−4.42
	IBP	−4.28	−4.35
	Tebufenozide	−4.44	−4.39
	Methoxyfenozide	−4.33	−4.38
	RH-5849	−4.34	−4.42

A  $\rightarrow$  B, apical to basolateral; B  $\rightarrow$  A, basolateral to apical.

## 2.5. Membrane retention

Since the membrane retention (%R) of the compounds was considered to be another factor which affects the permeability of hydrophobic compounds, %R was estimated and is listed in Table 1. The values of the membrane retention of the compounds with  $\log P_{\text{oct}} \leq 2$  and  $\log P_{\text{oct}} > 2$  were 0.3–20% and 0–69%, respectively. The values of %R tended to increase with the increase of  $\log P_{\text{oct}}$ .

## 2.6. Caco-2 cell permeability

Table 4 shows the logarithm of the Caco-2 cell permeability coefficients of chemicals and agrochemicals. The apical to basolateral permeability of all tested compounds was similar to the basolateral to apical permeability, suggesting that the tested chemicals and agrochemicals were mainly transported passively through the Caco-2 cell monolayers.

## 3. Discussion

### 3.1. Permeability with artificial membranes of hydrophobic compounds

It is important to predict the oral absorption of hydrophobic compounds from the perspective of not only effective screening for drug candidates in the early drug discovery stage but also risk assessment for agrochemicals and endocrine-disrupting chemicals in the environment. In the present study, we measured the PAMPA permeability coefficients of hydrophobic compounds which are useful for the prediction of human intestinal absorption.

The measured  $\log P_{\text{app-pampa}}$  values of added hydrophobic compounds in this study were lower than the calculated values as well as of imipramine, desipramine, and testosterone in the previous study. As shown in Figure 1, the measured  $\log P_{\text{app-pampa}}$  value reached the maximum when the calculated  $\log P_{\text{app-pampa}}$  value was approximately −4.5. The peak value of −4.5 was similar to the  $\log P_{UWL}$  values (−4.95 to −4.44; Table 3) estimated by the pH dependence method. This indicates that the value of −4.5 implies a limitation of permeability by the UWL, causing a difference between calculated and

measured values. In the range of the calculated  $\log P_{\text{app-pampa}}$  value ( $>-4.5$ ), the measured  $\log P_{\text{app-pampa}}$  values decreased with an increase of the calculated  $\log P_{\text{app-pampa}}$  value due to membrane retention (%R).

### 3.2. Classical QSAR equations for the $\log P_{\text{app-pampa}}$

To derive a new QSAR equation, we examined (1) adding new physicochemical parameter(s) which influence the permeability coefficients of hydrophobic compounds and (2) constructing a new QSAR model.

**3.2.1. Physicochemical parameters.** We attempted to find out other factor(s) for determining the permeability of hydrophobic compounds. As described in Section 3.1, the PAMPA permeability of hydrophobic compounds was affected by the UWL and membrane retention (%R). With regard to the UWL, it was anticipated that the diffusion property may be a factor in QSAR analyses. One good descriptor for the diffusion property is the (logarithm of) molecular weight (*MW*) because of an inverse relation between the diffusion coefficient and molecular weight. Ruell et al. showed the relationship between  $\log P_{\text{UWL}}$  and  $\log MW$  as the following Eq. 6:<sup>21</sup>

$$\log P_{\text{UWL}} = -3.72 - 0.41 \times \log MW. \quad (6)$$

However, *MW* or  $\log MW$  was not significant in analyzing variations in PAMPA permeability of hydrophobic compounds. A possible reason is that the range of *MW* in the dataset (93–455) corresponds with the narrow range of  $\log P_{\text{UWL}}$  values ( $-4.5$  to  $-4.8$ ) according to Eq. 6, resulting in insufficient evaluation of the relationship between apparent PAMPA permeability and  $\log MW$ .

Another factor which influences PAMPA permeability of hydrophobic compounds is membrane retention (%R). As presented in Table 1, %R showed an increasing tendency with the increase of  $\log P_{\text{oct}}$ . Avdeef et al. also reported that  $\log \%R$  were correlated with  $\log P_{\text{oct}}$ .<sup>12</sup> As a result of our preliminary QSAR analyses of the %R related parameter, other physicochemical parameters were insignificant. Thus, we formulated a QSAR equation for Groups 1 and 2 using the same physicochemical parameters as in the previous study. The Eq. 2 for Group 1 (calculated  $\log P_{\text{app-pampa}} \leq -4.5$ ) was comparable to Eq. 1 suggesting that Eqs. 1 and 2 were good prediction models for PAMPA permeability of non-hydrophobic compounds. In Eq. 3 for Group 2 (calculated  $\log P_{\text{app-pampa}} > -4.5$ ), although significant parameters were only  $\log P_{\text{oct}}$  and  $|\text{p}K_{\text{a}} - \text{pH}|$  because of the small number of datasets, the possibility of analyzing the combined datasets of Groups 1 and 2 with the descriptors  $\log P_{\text{oct}}$ ,  $|\text{p}K_{\text{a}} - \text{pH}|$ ,  $SA_{\text{HA}}$ , and  $SA_{\text{HD}}$  was suggested.

**3.2.2. New QSAR model.** We adopted a bilinear model<sup>19</sup> with apparent hydrophobicity for the analysis of all tested compounds based on Figure 1 and Eqs. 2 and 3. The bilinear model is widely used as well as the parabolic model for the correlation of  $\log P$  and bioactivity. Both parabolic and bilinear models fit the experimental data well, but the real advantage of the bilinear model

lies in its compatibility with the many good linear equations.<sup>22</sup>

Bilinear analysis for the whole dataset with apparent hydrophobicity,  $\log P_{\text{app}}$ ,  $\log P_{\text{oct}} - 0.67|\text{p}K_{\text{a}} - \text{pH}|$ , was carried out, formulating a good QSAR Equation 4 including both hydrophilic and hydrophobic compounds. As discussed in details in the previous studies,<sup>6,23,24</sup> if the partition of the ion-pair complexes of ionizable compounds can be ignored, the distribution coefficient (apparent hydrophobicity) of compounds at a particular pH ( $\log D_{\text{oct}}$ ) is represented by the following Eq. 7:

$$\log D_{\text{oct}} = \log P_{\text{oct}} - |\text{p}K_{\text{a}} - \text{pH}| \quad (\text{for acid } \text{p}K_{\text{a}} \ll \text{pH} \text{ and for bases } \text{p}K_{\text{a}} \gg \text{pH}). \quad (7)$$

When the compound is an acid (AH),  $K_{\text{a}} = [\text{A}^-][\text{H}^+]/[\text{AH}]$ . That is,  $\text{p}K_{\text{a}} - \text{pH} = -\log([\text{A}^-]/[\text{AH}])$ . When the compound is a base, the situation is same. Therefore,  $|\text{p}K_{\text{a}} - \text{pH}|$  corresponds to the logarithm of [ionized form]/[unionized form] of ionizable compounds.

$$\log D_{\text{oct}} = \log P_{\text{oct}} - \log[\text{ionized form}]/[\text{unionized form}]. \quad (8)$$

From Eq. 8, apparent hydrophobicity should decrease with the slope of ‘one’ as the experimental pH is separate from the  $\text{p}K_{\text{a}}$  of the compound. However, if the ionized form of ionizable compounds penetrates the membrane as ion-pair complexes with counter-ions in buffer systems, the descending slope in the  $\text{pH} - \log D_{\text{oct}}$  profile could be more gradual than one. Since the  $\alpha$  value for  $\log P_{\text{app}}$  ( $= \log D_{\text{oct}}$  in this experiment), the minus quantity of the coefficient of the  $|\text{p}K_{\text{a}} - \text{pH}|$  term, 0.67, which was adopted based on the coefficients of the terms in Eq. 2, was significantly less than one, it is presumed that the ionized form somewhat penetrates the membrane as ion-pair complexes.

To certify the validity of the  $\alpha$  value, bilinear equations were derived with  $\alpha = 0.4, 0.5, 0.6, 0.7, 0.8, 0.9$  and the quality of the equations was compared. Table 5 shows the  $s$ ,  $r^2$ , and  $q^2$  of the bilinear equations. Although the difference of  $s$ ,  $r^2$ , and  $q^2$  is small, it is obvious that the optimized  $\alpha$  value is between 0.6 and 0.7. Therefore, ‘0.67’ obtained from Eq. 2 was adopted as the value of  $\alpha$ . Note that the value of 0.67 determined by the experiment in this study is anticipated to depend on buffer systems and components of membranes, because different

**Table 5.**  $s$ ,  $r^2$ , and  $q^2$  values in the bilinear equations derived with different  $\alpha$  values

$\alpha$	$s$	$r^2$	$q^2$
0.4	0.387	0.686	0.644
0.5	0.371	0.712	0.672
0.6	0.363	0.723	0.684
0.67 <sup>a</sup>	0.363	0.724	0.684
0.7	0.364	0.723	0.683
0.8	0.366	0.719	0.679
0.9	0.378	0.700	0.657

<sup>a</sup> From Eq. 4.



kinds and concentrations of ion-pair complexes would be formed.

### 3.3. The effect of the UWL on QSAR equations for permeability

The coefficient of  $\log P_{\text{oct}}$  in Eq. 5 for intrinsic permeability,  $\log P_0$ , was 1.34, which is not far from unity, whereas the coefficient of  $\log P_{\text{oct}}$  was 0.43, 0.42, and 0.53, significantly less than unity, in Eqs. 1, 2, and 4 for  $\log P_{\text{app-pampa}}$ , respectively. For partition coefficients in different solvents from 1-octanol and water system,  $\log P_{\text{solv}}$ , the following equation is generalized.<sup>6,25</sup>

$$\log P_{\text{solv}} = \log P_{\text{oct}} + \Delta \log f(\text{HB}) + \text{const.} \quad (9)$$

In Eq. 9, the  $\Delta \log f(\text{HB})$  term relates to the difference of the hydrogen bonding capability of compounds for a solvent and 1-octanol. Since  $\log P_0$  is the intrinsic partition coefficient in the artificial membranes and water system, a type of  $\log P_{\text{solv}}$ , the coefficient of the  $\log P_{\text{oct}}$  term in Eq. 5 should be unity. The UWL acts as a rate-limiting barrier for PAMPA permeability of hydrophobic compounds, resulting in a lower slope of  $\log P_{\text{oct}}$  in Eqs. 1, 2, and 4, whereas  $\log P_0$  is not affected by the UWL. The coefficient, 1.34, approximates to the coefficient of  $\log P_{\text{oct}}$ , 1.31, in the equation formulated for PAMPA permeability obtained using the 2% DOPC/dodecane system.<sup>12</sup>

### 3.4. Relationship between PAMPA permeability and Caco-2 permeability/human oral absorption

In the previous study, we reported the relationship between Caco-2 cell permeability (apical to basolateral direction) and the PAMPA permeability of seven peptide-related compounds<sup>5</sup> and 20 commercial drugs (Eq. 10);<sup>6</sup>

$$\log P_{\text{app-caco-2}} = 1.03 (\pm 0.21) \log P_{\text{app-pampa}} + 0.39 (\pm 1.10) \quad (10)$$

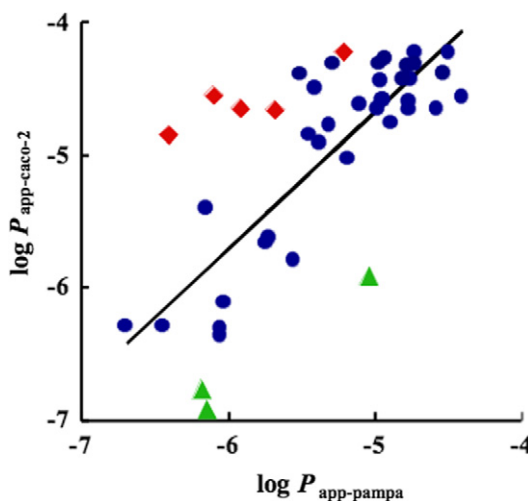
$$n = 27, s = 0.31, r^2 = 0.81, q^2 = 0.78.$$

Figure 4 represents the relationship between PAMPA and Caco-2 cell permeability coefficients of all compounds in this study. Eq. 11 was formulated for Caco-2 cell permeability coefficients of compounds mainly permeated by the passive transcellular route (seven peptide-related compounds,<sup>5</sup> 20 commercial drugs,<sup>6</sup> eight chemicals and agrochemicals), showing good correlation with PAMPA permeability coefficients.

$$\log P_{\text{app-caco-2}} = 1.03 (\pm 0.21) \log P_{\text{app-pampa}} + 0.49 (\pm 1.09) \quad (11)$$

$$n = 35, s = 0.35, r^2 = 0.76, q^2 = 0.73.$$

The slope and intercept values in Eq. 11 were almost the same as those in Eq. 10, respectively. Eq. 11 indicates that the Caco-2 cell permeability of hydrophobic compounds as well as peptide-related compounds and drugs is predictable from their PAMPA permeability. The maximum Caco-2 cell permeability was around  $-4.2$



**Figure 4.** The relationship between the Caco-2 cell and artificial membrane permeability coefficients of compounds, including compounds mainly permeated by the passive transcellular route (●), actively transported compounds (◆), and the compounds excreted by efflux system (▲).

in the experimental condition because of the UWL adjacent to Caco-2 cell surfaces. The UWL of Caco-2 cells ( $1544 \mu\text{m}^2$ ) is thinner than that of PAMPA membranes ( $2000\text{--}4000 \mu\text{m}^2$ ), resulting in a greater maximum value of Caco-2 cell permeability than that of PAMPA (around  $-4.5$ ).

It was reported that human intestinal absorption has a sigmoidal relationship with Caco-2 cell permeability.<sup>27</sup> We attempted to predict the human intestinal absorption of chlorpyrifos (an insecticide) using Eqs. 4 and 9. The  $\log P_{\text{app-pampa}}$  value of chlorpyrifos was calculated as  $-5.92$  using its parameter values ( $\log P_{\text{oct}} = 4.82$ ;  $|\text{p}K_{\text{a}} - \text{pH}| = 0$ ;  $S_{\text{A}_{\text{HA}}} = 0.477$ ;  $S_{\text{A}_{\text{HD}}} = 0$ ). The  $\log P_{\text{app-caco-2}}$  value of chlorpyrifos,  $-5.61$ , calculated from its  $\log P_{\text{app-pampa}}$ , corresponds to approximately 80% of the fraction absorbed after oral administration to humans according to the sigmoid graph in the report of Stenberg et al.<sup>27</sup> The estimated absorbed fraction of chlorpyrifos is comparable to its measured absorption rate after oral administration to humans (72%<sup>28</sup> or 93%<sup>29</sup>, average 83%). The result demonstrates that the QSAR equations formulated in this study are useful for the prediction of human exposure to hydrophobic compounds.

## 4. Conclusions

In this study, we clarified the barrier by the UWL on membrane surfaces and the membrane retention influencing PAMPA permeability of hydrophobic compounds. The bilinear QSAR model explained the PAMPA permeability of diverse compounds, whether hydrophilic or hydrophobic, with the same physicochemical parameters as those in the previous study. It was shown the PAMPA permeability is able to predict Caco-2 cell permeability, including hydrophobic compounds, which is used for the evaluation of human oral absorption. Although we also measured  $\log P_{\text{app-pampa}}$  under the stirred condition

to examine the effect of the UWL on the PAMPA permeability, it was difficult to remove completely the UWL even at the high stirring speed. Since the UWL exists adjacent to all membranes, the PAMPA permeability under the unstirred condition seems to be sufficient for the prediction of human oral absorption.

Many chemicals and agrochemicals are hydrophobic, and hydrophobic compounds generally have low solubility in water. Furthermore, some chemicals have neurologic, carcinogenic, pulmonary, and reproductive effects.<sup>30</sup> Therefore, it may be difficult to measure the PAMPA permeability of some hydrophobic compounds because of their low solubility and/or toxicological effects even if PAMPA is a good screening system for human oral absorption. In this situation, the bilinear equation for PAMPA permeability proposed in this study should be useful for *in silico* prediction of PAMPA. In conclusion, the bilinear model is applicable for not only effective screening for several drug candidates but also risk assessment of chemicals and agrochemicals absorbed by humans.

## 5. Experimental

### 5.1. Materials

Thirty-eight commercial drugs, 28 chemicals, and 11 agrochemicals were purchased from Nacalai Tesque (Kyoto, Japan), Kokusan Chemical Co. Ltd (Tokyo, Japan), Wako Pure Chemical Industries (Osaka, Japan), Bachem AG (Bubendorf, Switzerland), Kanto Chemical (Tokyo, Japan), Sigma–Aldrich Japan (Tokyo, Japan), Tocris Cookson Ltd (Bristol, UK) or BIOMOL Research Laboratories Inc. (PA, USA). Lecithin from egg yolk was purchased from Sigma (MO, USA). Hydrophobic filter plates (MultiScreen-IP, Clear Plates, 0.45  $\mu\text{m}$ -diameter pore size), 96-well microplates, and 96-well UV-transparent microplates (COSTAR UV-plate) were obtained from Millipore (MA, USA), Asahi Techno Glass Corp. (Osaka, Japan), and Corning (MA, USA), respectively. All other reagents were of analytical grade and were purchased from Wako Pure Chemical Industries.

### 5.2. Permeability experiments with artificial membranes

Permeability experiments of chemicals and agrochemicals were carried out according to the procedures developed by our previous study.<sup>6</sup> In brief, a 96-well microplate (acceptor compartment) was completely filled with Tris–HCl buffer (pH 7.3) containing 5–30% DMSO. A hydrophobic filter plate (donor compartment) was fixed on the buffer-filled plate. The filter surface was impregnated with 5  $\mu\text{L}$  of 10% (v/v) lecithin solution in 1,9-decadiene. A 125–500  $\mu\text{M}$  compound solution in the same buffer containing 5–30% DMSO was prepared depending upon the compound solubility. A 200  $\mu\text{L}$  sample of the compound solution was added to the filter plate and incubated at 25 °C for 2, 5 or 24 h. The filter plate was carefully removed and 200  $\mu\text{L}$  of the solution in the acceptor compartment was placed on a UV-transparent microplate. The con-

centration of the solution in the UV-plate was then determined by UV spectroscopy, using the microtiter plate reader (FLUOstar OPTIMA) at 260 or 280 nm. A reference solution defining equilibrium conditions was prepared at the same concentration as the sample solution with no membrane barrier. The filter surface was wetted with 5  $\mu\text{L}$  of a 60% (v/v) methanol/buffer solution as the reference. The permeability coefficient through the artificial membrane,  $P_{\text{app-pampa}}$ , was calculated using Eq. 12.<sup>11</sup>

$$P_{\text{app-pampa}} = -V_D V_R / [(V_D + V_R) A t] \cdot \ln(1 - \text{OD}_{\text{sam}} / \text{OD}_{\text{ref}}). \quad (12)$$

In this equation,  $V_D$  ( $\text{cm}^3$ ) is the donor volume (0.2  $\text{cm}^3$ ),  $V_R$  ( $\text{cm}^3$ ) is the volume of the acceptor compartment (0.38  $\text{cm}^3$ ),  $A$  ( $\text{cm}^2$ ) is the accessible filter area (0.283  $\text{cm}^2$ ), and  $t$  (s) is the incubation time.  $\text{OD}_{\text{sam}}$  and  $\text{OD}_{\text{ref}}$  are optical density (OD) at 260 or 280 nm of the sample and reference solutions in the acceptor compartment, respectively.

### 5.3. Permeability with artificial membranes under the stirred condition

The experimental condition was based on the method described in Section 5.2. An alumina ball (HD-3, AS ONE Corp., Japan) was set in a 96-well microplate (acceptor compartment) with a hydrophobic filter plate (donor compartment).<sup>31</sup> A 200  $\mu\text{L}$  sample of the compound solution was added to the filter plate and incubated at 25 °C for 20, 40, 80 min, 2 or 24 h. During incubation the filter plate was stirred at 250 rpm (or 100, 200 rpm) using a Multi-shaker mms (TOKYO RIKAKIKAI Co., Ltd, Japan) or ROTER MAX 120 (Heidolph Instruments, Germany). The permeability coefficient through the artificial membrane under the stirred condition,  $P_{\text{app-pampa (stir)}}$ , was calculated according to Eq. 12.

### 5.4. Unstirred water layer permeability and intrinsic permeability

Based on the method described in Section 5.2, we measured  $P_{\text{app-pampa}}$  of aminopyrine, diltiazem, alprenolol, metoprolol, propranolol, desipramine, imipramine, verapamil, ketoprofen, ibuprofen, salicylic acid, naproxen, piroxicam, and testosterone at pH 3–10. The 0.1 M phosphate buffer containing 5% DMSO (pH 3–10) was used as the solution in the acceptor and donor compartments. The unstirred water layer permeability coefficients,  $P_{\text{UWL}}$ , and the ‘flux’ ionization constant,  $\text{p}K_{\text{a}}^{\text{flux}}$ , were evaluated by fitting the data of Figure 3 to Eq. 13<sup>21</sup> using the least squares method with WinNonlin software version 5.0.1.<sup>32</sup> The intrinsic permeability coefficient,  $P_0$ , was calculated from  $\log P_{\text{UWL}}$  and  $\text{p}K_{\text{a}}^{\text{flux}}$  using Eq. 14.<sup>21</sup>

$$\log P_{\text{app-pampa}} = \log P_{\text{e}}^{\text{max}} - \log(10^{\pm(\text{pH} - \text{p}K_{\text{a}}^{\text{flux}})} + 1). \quad (13)$$

$P_{\text{e}}^{\text{max}}$ : maximum effective PAMPA permeability coefficient

If  $P_0 \gg P_{\text{UWL}}$ ,  $\log P_{\text{e}}^{\text{max}} \approx \log P_{\text{UWL}}$ .

$$\log P_0 = \log P_{\text{UWL}} + |\text{p}K_{\text{a}} - \text{p}K_{\text{a}}^{\text{flux}}|. \quad (14)$$

### 5.5. Membrane retention

The concentrations of the compound in both acceptor and donor compartments were determined using the microtiter plate reader (FLUOstar OPTIMA) in the permeability experiment with artificial membranes. The membrane retention (%*R*) was calculated from the obtained concentrations and Eq. 15.<sup>12</sup>

$$\%R = (R_{\text{ref}} - R_{\text{sam}}) \times 100, \quad (15)$$

$R_{\text{sam}}$  = the total amount of compounds in acceptor and donor compartments (sample solution)/the applied amount of compounds in the donor compartment (sample solution),

$R_{\text{ref}}$  = the total amount of compounds in acceptor and donor compartments (reference solution)/the applied amount of compounds in the donor compartment (reference solution).

### 5.6. Caco-2 cell permeability

Caco-2 cell permeability experiments of chemicals and agrochemicals (diphenylamine, atrazine, diazinon, DMTP, IBP, tebufenozide, halofenozide, and RH-5849) were carried out by Absorption Systems LP (PA, USA). Confluent monolayers of Caco-2 cells (21–28 days old) were prepared in Transwell assay plates. The apparent Caco-2 permeability coefficient at pH 7.4 ± 0.2 in both directions (apical to basolateral and basolateral to apical) was measured. Five micromolar of a test compound in Hanks' balanced salt solution with maximum DMSO concentration less than 1% was dosed on the apical or basolateral side. The concentrations of the test compound on both apical and basolateral sides at 2 h after dosing were determined using LC/MS. Caco-2 cell permeability coefficients were then determined by the standard method.<sup>4</sup>

### 5.7. The partition coefficient $P_{\text{oct}}$ and the dissociation constant $K_a$

For the log  $P_{\text{oct}}$  value, the measured values were available from the database of MacLogP software, version 4.0.<sup>22,33</sup> Their  $\text{p}K_a$  values were obtained from the CQSAR Database.<sup>34</sup> The absolute value of the difference between the  $\text{p}K_a$  value of the compound and the experimental pH 7.3,  $|\text{p}K_a - \text{pH}|$ , was used for QSAR analyses as a descriptor. The log  $P_{\text{oct}}$  and  $|\text{p}K_a - \text{pH}|$  values are listed in Table 1.

### 5.8. Molecular modeling

All computations were performed using the molecular modeling software package SYBYL, version 6.9.<sup>35</sup> To select the initial conformation of compounds, we started from the coordinates of X-ray crystallographic data for each compound obtained from the Cambridge Structure Database,<sup>36</sup> if available. The X-ray structure of each compound was geometry optimized by the Tripos force field to give a relatively stable conformer. The coordi-

nates of the modified parts of these structures were calculated using the SYBYL standard values for bond lengths and angles. A systematic search in SYBYL was applied to all rotatable bonds. The low-energy conformer of each compound obtained by a systematic search was then geometry optimized by the Tripos force field. All compounds were modeled in their neutral form.

### 5.9. Surface area calculations

MOLPROP in SYBYL was used to calculate the surface area occupied by the hydrogen-bond acceptor and donor atoms of each modeled conformer ( $SA_{\text{HA}}$  and  $SA_{\text{HD}}$  [ $\text{\AA}^2 \times 1/100$ ], respectively). The hydrogen-bond acceptor atoms were defined as nitrogen and oxygen atoms, while the hydrogen-bond donor atoms were defined as hydrogen atoms attached to these heteroatoms.

### 5.10. Classical QSAR

PAMPA permeability, log  $P_{\text{app-pampa}}$ , was quantitatively analyzed using the classical QSAR technique. Classical QSAR analyses were performed with QREG, version 2.05.<sup>37</sup> Bilinear analysis was carried out with CQSAR software.<sup>34</sup>

### Acknowledgments

We are grateful to Nippon Kayaku Co., Ltd and Sankyo Agro Co., Ltd for providing a test compound, chromafenozide, and Dr. Yoshiaki Nakagawa (Kyoto University) for providing compounds, tebufenozide, methoxifenozide, and halofenozide. We also thank Emeritus Professor Toshio Fujita (Kyoto University) and Dr. Kiyohiko Sugano (Pfizer Japan Inc.) for helpful advice and comments on QSAR, and advice on the permeability experiment, respectively. The Caco-2 cell permeability coefficients of diphenylamine, atrazine, diazinon, DMTP, IBP, tebufenozide, halofenozide, and RH-5849 were measured by Absorption Systems LP (PA, USA). This work was supported in part by a Grant-in Aid for Scientific Research (16510158) from the Ministry of Education, Culture, Sports, Science and Technology of Japan.

### References and notes

- Lin, J.; Sahakian, D. C.; de Moraes, S. M. F.; Xu, J. J.; Polzer, R. J.; Winter, S. M. *Curr. Topics Med. Chem.* **2003**, *3*, 1125.
- Kansy, M.; Senner, F.; Gubernator, K. *J. Med. Chem.* **1998**, *41*, 1007.
- Zhu, C.; Jiang, L.; Chen, T. M.; Hwang, K. K. *Eur. J. Med. Chem.* **2002**, *37*, 399.
- Ano, R.; Kimura, Y.; Urakami, M.; Shima, M.; Matsuno, R.; Ueno, T.; Akamatsu, M. *Bioorg. Med. Chem.* **2004**, *12*, 249.
- Ano, R.; Kimura, Y.; Shima, M.; Matsuno, R.; Ueno, T.; Akamatsu, M. *Bioorg. Med. Chem.* **2004**, *12*, 257.
- Fujikawa, M.; Ano, R.; Nakao, K.; Shimizu, R.; Akamatsu, M. *Bioorg. Med. Chem.* **2005**, *13*, 4721.

7. Sugano, K.; Hamada, H.; Machida, M.; Ushio, H. *J. Biomol. Screen* **2001**, 6, 189.
8. Sugano, K.; Takata, N.; Machida, M.; Saitoh, K.; Terada, K. *Int. J. Pharm.* **2002**, 241, 241.
9. Sugano, K.; Nabuchi, Y.; Machida, M.; Aso, Y. *Int. J. Pharm.* **2003**, 257, 245.
10. Di, L.; Kerns, E. H.; Fan, K.; McConnel, O. J.; Carter, G. T. *Eur. J. Med. Chem.* **2003**, 38, 223.
11. Wohnsland, F.; Faller, B. *J. Med. Chem.* **2001**, 44, 923.
12. Avdeef, A. In *Absorption and Drug Development*; Wiley-Interscience: New Jersey, 2003.
13. Bermejo, M.; Avdeef, A.; Ruiz, A.; Nalda, R.; Ruell, J. A.; Tsinman, O.; González, I.; Fernández, C.; Sánchez, G.; Garrigues, T. M.; Merino, V. *Eur. J. Pharm. Sci.* **2004**, 21, 429.
14. Avdeef, A.; Artursson, P.; Neuhooff, S.; Lazorova, L.; Gråsjö, J.; Tavelin, S. *Eur. J. Pharm. Sci.* **2005**, 24, 333.
15. Kerns, E. H.; Di, L.; Petusky, S.; Farris, M.; Ley, R.; Jupp, P. *J. Pharm. Sci.* **2004**, 93, 1440.
16. Corti, G.; Maestrelli, F.; Cirri, M.; Zerrouk, N.; Mura, P. *Eur. J. Pharm. Sci.* **2006**, 27, 354.
17. Ottaviani, G.; Martel, S.; Carrupt, P. A. *J. Med. Chem.* **2006**, 49, 3948.
18. Alavanja, M. C. R.; Hoppin, J. A.; Kamel, F. *Annu. Rev. Public. Health* **2004**, 25, 155.
19. Kubinyi, H. *J. Med. Chem.* **1977**, 20, 625; Kubinyi, H. *Arzneim.-Forsch.* **1979**, 29, 1067.
20. Avdeef, A.; Nielsen, P. E.; Tsinman, O. *Eur. J. Pharm. Sci.* **2004**, 22, 365.
21. Ruell, J. A.; Tsinman, K. L.; Avdeef, A. *Eur. J. Pharm. Sci.* **2003**, 20, 393.
22. Hansch, C.; Leo, A. In *Exploring QSAR*; American Chemical Society: Washington, DC, 1995.
23. Fujita, T.; Hansch, C. *J. Med. Chem.* **1967**, 10, 991.
24. Terada, H.; Kitagawa, K.; Yoshikawa, Y.; Kametani, F. *Chem. Pharm. Bull.* **1981**, 29, 7.
25. Fujita, T.; Nishioka, T.; Nakajima, M. *J. Med. Chem.* **1977**, 20, 1071.
26. Karlsson, J. P.; Artursson, P. *Int. J. Pharm.* **1991**, 71, 55.
27. Stenberg, P.; Norinder, U.; Luthman, K.; Artursson, P. *J. Med. Chem.* **2001**, 44, 1927.
28. Nolan, R. J.; Rick, D. L.; Freshour, N. L.; Saunders, J. H. *Toxicol. Appl. Pharmacol.* **1984**, 73, 8.
29. Griffin, P.; Mason, H.; Heywood, K.; Cocker, J. *Occup. Environ. Med.* **1999**, 56, 10.
30. Dennis, D.; Weisenburger, MD. *Human Pathol.* **1993**, 24, 571.
31. Sugano, K. Personal communication.
32. WinNonlin version 5.0.1; Pharsight Corp.: Mountain View, CA, USA.
33. MacLogP 4.0; Biobyte Corp.: Claremont, CA, USA.
34. CQSAR; Biobyte Corp.: Claremont, CA, USA.
35. SYBYL Molecular Modeling Software; Tripos Associates, Inc.: St Louis, MO, USA.
36. The Cambridge Structural Database; CCSD: Cambridge, UK.
37. Asao, M.; Shimizu, R.; Nakao, K.; Nishioka, T.; Fujita, T. QREG 2.05: Japan Chemistry Program Exchange: Ibaraki, Japan.
38. Yazdanian, M.; Glynn, S. L.; Wright, J. L.; Hawi, A. *Pharm. Res.* **1998**, 15, 1490.